An Intrinsic Analysis of Human Brucellosis Dynamics in Africa

Paride O. Lolika [a*] and Mlyashimbi Helikumi [b]

[a]*Department of Mathematics, University of Juba, P.O. Box 82 Juba, Central Equatoria, South Sudan.*

[b] *Department of Mathematics and Statistics, College of Science and Technical Education, Mbeya University of Science and Technology, P.O. Box-131, Mbeya, Tanzania.*

Author's contributions

This work was carried out in collaboration between both authors. Both authors read and approved the final manuscript.

Original Research Article

Abstract

Brucellosis is one of the most common zoonotic infections globally. It affects humans, domestic animals and wildlife. In this paper, we conduct an intrinsic analysis of human brucellosis dynamics in non-periodic and periodic environments. As such we propose and study two mathematical models for human brucellosis transmission and control, in which humans acquire infection from cattle and wildlife. The first model is an autonomous dynamical system and the second is a non-autonomous dynamical system in which the seasonal transmission of brucellosis is incorporated. Disease intervention strategies incorporated in this study are cattle vaccination, culling of infectious cattle and human treatment. For both models we conduct both epidemic and endemic analysis, with a focus on the threshold dynamics characterized by the basic reproduction numbers. Using sensitivity analysis we established that $\mathcal{R}_0$ is most sensitive to the rate of brucellosis transmission from buffalos to cattle, the result suggest that in order to control human brucellosis there is a need to control cattle infection. Based on our models, we also formulate an optimal control problem with cattle vaccination and culling of infectious cattle as control functions. Using reasonable parameter values, numerical simulations of the optimal control demonstrate the possibility of reducing brucellosis incidence in humans, wildlife and cattle, within a finite time horizon, for both periodic and non-periodic environments.

*Corresponding author: E-mail: parideoresto@yahoo.com;

1   Introduction

Globally, human brucellosis remains an important and widespread infection [1]. The infection is more common in Mediterranean areas, the south and the center of America, Africa, Asia, Arab peninsula, Indian subcontinent and the Middle East [2]. In 2012, reported brucellosis incidence in some endemic regions were as follows: Saudi Arabia (214.4), Iran (238.6), Turkey (262.2), Iraq (278.4), and Syria (1603.4) [3]. However, the World Health Organization (WHO) believes that the real incidence is 10–25 times more than what have been reported [2]. Although, human brucellosis in rampant in many developing nations it is also a severe public health problem in China where 160, 214 brucellosis cases were observed in the period 2005–2010 [4].

In animals, brucellosis is transmitted by direct contact transmission through the brucella carriers or indirect contact transmission when animals ingest contaminated forages or the excrement containing large quantities of bacteria, generally discharged by infected animals [5]. Domesticated species such as cattle, sheep, horse and goats are regarded as the main source of human brucellosis [2], in which transmission may occur directly or through the consumption of unpasteurised dairy products [5]. The cross-transmission of brucellosis between domesticated animals and wildlife is well documented [6, 7]. However, the debate on whether wildlife is the reservoir of infection for domestic animals or vice versa continues [6]. One wild animal that is a villain for inter-species spread of many infectious disease such as brucellosis, foot-and-mouth disease-virus (FMDV) in many Africa nations is the African buffalo [6]. African buffaloes have several intrinsic behavioural characteristics which are key to inter-species spread of infectious diseases. They are highly mobile and sociable species and they often move in large herds of 1000 or more [8].

Recently, a number of veterinary scientists have suggested that buffalo, a preferred source of bush meat could be another source of human brucellosis in many developing nations [6]. Buffalo meat is highly preferred bush meat in many African countries [9]. Since bush meat is consumed and handled (legally and illegally) in many developing nations its contribution to human brucellosis cannot be ignored.

Several mathematical models have been proposed to study the dynamics of brucellosis outbreaks [5, 10, 11, 12, 13, 14, 15, 16, 17, 18, 19, 20, 21, 22, 23, 24, 25, 26]. Undeniably, these studies have produced many useful results and improved the existing knowledge on brucellosis dynamics. One of the limitations of these models, however, is that none of them incorporated the aspect of bush meat on modeling the transmission dynamics of human brucellosis. In this paper we develop a novel mathematical model that evaluates the impact of bush meat on human brucellosis dynamics. Our model will incorporate human population, cattle and wildlife (African buffalo). In addition, we will explore optimal disease control measures based on cattle vaccination, culling of infectious cattle and treatment of infected humans.

The remainder of this paper is organized as follows. In section 2 we formulate and comprehensively analyze the transmission dynamics of brucellosis in non-periodic environments. We provide sensitivity analysis of the basic reproductive number on various model parameters in non-periodic environments, identifying the parameters to which reproductive number is most sensitive, we use this information to suggest strategies for controlling brucellosis using techniques from optimal control theory. We extend the autonomous brucellosis models formulated to incorporate seasonal variations on disease transmission. We then conduct mathematical analyses, including the computation of the basic

reproductive number, and the stability analysis of equilibria. We formulate an optimal control problem with cattle vaccination and culling of infectious cattle as control functions. Finally, a brief discussion in Section 3 rounds up the paper.

2 Materials and Methods

2.1 An autonomous brucellosis model

We propose an autonomous dynamical system that comprise of cattle population, human population and African buffalo population. The African buffalo population constitute three compartments: susceptible $S_b(t)$, symptomatic infectious $I_b(t)$ and carrier state - asymptomatic persistent infection $A(t)$. Thus the total population of buffaloes at time t is $N_b(t) = S_b(t) + I_b(t) + A(t)$. The cattle population is subdivided into classes of: susceptible $S_c(t)$, infectious $I_c(t)$, and the total cattle population at time t is $N_c(t) = S_c(t) + I_c(t)$. Further, the human population constitute: susceptible $S_h(t)$ and infectious $I_h(t)$. The total human population at time t is $N_h(t) = S_h(t) + I_h(t)$. There are some assumptions for our model:

1. Brucellosis in the exposure period is hardly detected, and animals in this period can also infect susceptible animal and humans. Hence, we ignored the exposed/latent period in both human and animal population (see for example [15, 20, 21, 22]);

2. Prior studies suggest that African buffaloes have more chances of becoming chronic carriers of the disease [6, 27]. As such we omitted the carrier compartment on describing brucellosis transmission dynamics in cattle and humans;

3. Here, brucellosis transmission rate is being modeled by the mass action incidence since it is appropriate when $N(t)$ is not too large [28]. We assume that the transmission rate is dependent on the size of the population which implies that the contact rate is an increasing function of the population. The mass action incidence is density- dependent since contact rate per infective is proportional to the density of the infectious host.

In all the discussions to follow we will denote the African buffalo, cattle and human by subscripts b, c and h, respectively. A flow diagram describing the model is given in Fig.1 and the model equations are:

$$\begin{cases} \frac{dS_b}{dt} = \Lambda_b - [\beta_{bb}(I_b + \epsilon A) + \beta_{cb}I_c]S_b - \mu_b S_b, \\ \frac{dI_b}{dt} = [\beta_{bb}(I_b + \epsilon A) + \beta_{cb}I_c]S_b - [\mu_b + \gamma]I_b, \\ \frac{dA}{dt} = f\gamma I_b - [\mu_b + d_b]A, \\ \frac{dS_c}{dt} = \Lambda_c - [\beta_{bc}(I_b + \epsilon A) + \beta_{cc}I_c]S_c - [\sigma + \mu_c]S_c, \\ \frac{dI_c}{dt} = [\beta_{bc}(I_b + \epsilon A) + \beta_{cc}I_c]S_c - [\mu_c + d_c]I_c, \\ \frac{dS_h}{dt} = \Lambda_h - \beta_{bh}(I_b + \epsilon A)S_h - \beta_{ch}I_c S_h - \mu_h S_h + \theta I_h, \\ \frac{dI_h}{dt} = \beta_{bh}(I_b + \epsilon A)S_h + \beta_{ch}I_c S_h - (\theta + \mu_h)I_h, \end{cases} \tag{1}$$

In system (1), Λ_i denote the constant recruitment rate into the population through birth, μ_i is the natural-related death rate $(i = b, c, h)$, d_b is the disease-related mortality rate for buffalo population, $d_c = \alpha + \delta$, where α is the culling rate and δ is the disease-related mortality rate, σ is the vaccination rate, ϵ accounts for the unequal chances of disease transmission between symptomatic and asymptomatic buffaloes, β_{ij} $(i, j = b, c)$ denotes disease transmission rate, with $i = j$ implying buffalo–to–buffalo or cattle–to–cattle transmission and $i \neq j$ signify cross-transmission, respectively, β_{bh} and β_{ch} denotes transmission rate from buffalo and cattle, respectively, to humans. Further, infected African buffaloes display clinical signs of the disease for γ^{-1} days after which a fraction f become chronic carriers and the complementary $(1 - f)$ succumb to disease-related death. Infected human displaying clinical signs of the disease are treated at rate θ. Prior studies suggests that the optimal treatment of uncomplicated brucellosis should be based on a six-week regimen of doxycycline

combined either with streptomycin for 2–3 weeks, or rifampicin for six weeks [29].

Although, species can be infected by the brucella through indirect transmission (environmental transmission), prior studies suggests that this form of infection plays a relatively small role on the spread of brucellosis [11, 14]. In addition, prior studies also suggests that humans rarely transmit the disease [11, 14].
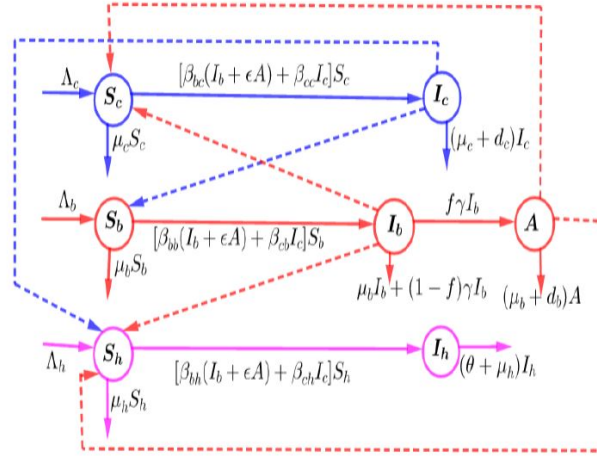

Fig. 1. Flow diagram representing the transmission routes and other processes model by system (1).

Since the last two equations are independent of the first five equations of model (1), without loss of generality, in our mathematical analysis we will consider only the first five equations :

$$
\begin{cases}
\frac{dS_b}{dt} = \Lambda_b - [\beta_{bb}(I_b + \epsilon A) + \beta_{cb}I_c]S_b - \mu_b S_b, \\
\frac{dI_b}{dt} = [\beta_{bb}(I_b + \epsilon A) + \beta_{cb}I_c]S_b - [\mu_b + \gamma]I_b, \\
\frac{dA}{dt} = f\gamma I_b - [\mu_b + d_b]A, \\
\frac{dS_c}{dt} = \Lambda_c - [\beta_{bc}(I_b + \epsilon A) + \beta_{cc}I_c]S_c - [\sigma + \mu_c]S_c, \\
\frac{dI_c}{dt} = [\beta_{bc}(I_b + \epsilon A) + \beta_{cc}I_c]S_c - [\mu_c + d_c]I_c.
\end{cases}
\tag{2}
$$

It can easily be verified that model (2) has a unique and bounded solutions with initial value in $\mathbb{R}_+^5$. Further, the compact set

$$
\Gamma = \left\{ (S_b, I_b, A, S_c, I_c) \in \mathbb{R}_+^5 : N_b \le \frac{\Lambda_b}{\mu_b}, \quad N_c \le \frac{\Lambda_c}{\mu_c}. \right\},
\tag{3}
$$

is positively invariant and attracting with respect to model (2).

2.1.1   The reproductive number

It is evident that (2) always has a disease-free equilibrium (DFE) given by

$$
\mathcal{E}^0 : \left[S_b^0, I_b^0, A^0, S_c^0, I_c^0 \right] = \left[\frac{\Lambda_b}{\mu_b}, 0, 0, \frac{\Lambda_c}{(\sigma + \mu_c)}, 0 \right].
$$

One measure of the severity of a disease is the basic reproductive number, $\mathcal{R}_0$, which is defined as the average number of secondary infections caused by a single infected animal in a completely susceptible population. Using the second generation matrix approach [30], the non-negative matrix

F that denotes the generation of new infection terms and the non-singular matrix V that denotes the remaining transfer terms are respectively, given (at the disease-free equilibrium) by

$$F = \begin{bmatrix} \frac{\beta_{bb}\Lambda_b}{\mu_b} & \frac{\epsilon\beta_{bb}\Lambda_b}{\mu_b} & \frac{\beta_{cb}\Lambda_b}{\mu_b} \\ 0 & 0 & 0 \\ \frac{\beta_{bc}\Lambda_c}{(\sigma+\mu_c)} & \frac{\epsilon\beta_{bc}\Lambda_c}{(\sigma+\mu_c)} & \frac{\beta_{cc}\Lambda_c}{(\sigma+\mu_c)} \end{bmatrix}, \quad \text{and} \quad V = \begin{bmatrix} (\mu_b+\gamma) & 0 & 0 \\ -f\gamma & (\mu_b+d_b) & 0 \\ 0 & 0 & (\mu_c+d_c) \end{bmatrix}. \quad (4)$$

Thus, the next generation matrix of system (2) is

$$FV^{-1} = \begin{bmatrix} M_{11} & M_{12} & M_{13} \\ M_{21} & M_{22} & M_{23} \\ 0 & 0 & 0 \end{bmatrix},$$

where

$$\begin{cases} M_{11} &= \dfrac{\Lambda_b\beta_{bb}}{(\mu_b+\gamma)\mu_b} + \dfrac{f\gamma\Lambda_b\epsilon\beta_{bb}}{(\mu_b+\gamma)(\mu_b+d_b)\mu_b}, \\[2mm] M_{21} &= \dfrac{\Lambda_c\beta_{bc}}{(\mu_b+\gamma)(\sigma+\mu_c)} + \dfrac{f\gamma\Lambda_c\epsilon\beta_{bc}}{(\mu_b+\gamma)(\mu_b+d_b)(\sigma+\mu_c)}, \\[2mm] M_{12} &= \dfrac{\Lambda_b\epsilon\beta_{bb}}{\mu_b(\mu_b+d_b)}, \quad M_{22} = \dfrac{\Lambda_c\epsilon\beta_{bc}}{(\sigma+\mu_c)(\mu_b+d_b)}, \\[2mm] M_{13} &= \dfrac{\Lambda_b\beta_{cb}}{\mu_b(\mu_c+d_c)}, \quad M_{23} = \dfrac{\Lambda_c\beta_{cc}}{(\sigma+\mu_c)(\mu_c+d_c)}. \end{cases}$$

It follows that the basic reproductive number is

$$\mathcal{R}_0 = \rho(FV^{-1}) = \frac{M_{11} + M_{22} + \sqrt{(M_{11}-M_{22})^2 + 4M_{12}M_{21}}}{2},$$

Defining the appropriate value of $\mathcal{R}_0$ for a disease characterized by hidden infections is challenging but essential in developing control measures. The reproductive number is the key threshold parameter whose values determine the global dynamics of system (2). A disease is considered to be endemic if $\mathcal{R}_0 > 1$. However, if $\mathcal{R}_0 \leq 1$ it implies that the disease dies out.

2.1.2   Equilibrium analysis

Theorem 2.1. *If $\mathcal{R}_0 \leq 1$, the system (2) has a unique DFE that is globally asymptotically stable in the region Γ.*

Proof. Let $\mathcal{Y}(t) = [I_b(t), A(t), I_c(t)]$. Since

$$\begin{cases} \dot{I}_b &\leq [\beta_{bb}(I_b+\epsilon A) + \beta_{cb}I_c]S_b^0 - [\mu_b+\gamma]I_b, \\ \dot{A} &\leq f\gamma I_b - [\mu_b+d_b]A, \\ \dot{I}_c &\leq [\beta_{bc}(I_b+\epsilon A) + \beta_{cc}I_c]S_c^0 - [\mu_c+d_c]I_c, \end{cases} \quad (5)$$

it follows that

$$\dot{\mathcal{Y}} \leq (F - V)\mathcal{Y},$$

where F and V are defined in Eq. (4). One can easily deduce that, both F and V^{-1} are non-negative. By the Perron-Frobenius Theorem, the non-negative matrix $V^{-1}F$ has a non-negative

left eigenvector $w \geq 0$ with respect to $\rho(V^{-1}F) = \rho(FV^{-1}) = \mathcal{R}_0$, that is $w^T V^{-1} F = \mathcal{R}_0 w^T$. Motivated by [31], we define a Lyapunov function as follows:

$$\mathcal{L} = w^T V^{-1} \mathcal{y}.$$

Differentiating $\mathcal{L}$ along solutions of (2), we have

$$\dot{\mathcal{L}} = w^T V^{-1} \dot{\mathcal{y}} \leq w^T V^{-1}(F - V)\mathcal{y} = (\mathcal{R}_0 - 1)w^T \mathcal{y}.$$

If $\mathcal{R}_0 < 1$, $\dot{\mathcal{L}} = 0$ implies that $w^T \mathcal{y} = 0$ and hence $I_b = A = I_c = 0$. It follows from the first and fourth equations of (2) that $S_b = S_b^0$ and $S_c = S_c^0$. Hence, the only invariant set where $\dot{\mathcal{L}} = 0$ is the singleton $\{S_b^0, 0, 0, S_c^0, 0\}$. By LaSalle's invariance principle [32], the DFE is globally asymptotic all stable in Γ if $\mathcal{R}_0 < 1$.

If $\mathcal{R}_0 = 1$, $\dot{\mathcal{L}} = 0$ implies that $S_b = S_b^0$ and $S_c = S_c^0$, by the first and third equations of (5) and the fact that $w^T \mathcal{y} > 0$. Then, from the first and fourth equations of (2) we have, $[\beta_{bb}(I_b + \epsilon A) + \beta_{cb}I_c]S_b = 0$ and $[\beta_{bc}(I_b + \epsilon A) + \beta_{cc}I_c]S_c = 0$, respectively. This can only happen if $I_b = A = I_c = 0$. Therefore, the largest invariant set where $\dot{\mathcal{L}} = 0$ is the singleton $\{S_b^0, 0, 0, S_c^0, 0\}$, and by LaSalle's invariance principle, the DFE is globally asymptotic all stable in Γ if $\mathcal{R}_0 = 1$. $\square$

Theorem 2.2. *If $\mathcal{R}_0 > 1$, there exists a unique endemic equilibrium of the system (2) which is globally asymptotically stable in the region Γ.*

Proof. In order to analyze the global asymptotic stability of the endemic equilibrium of system (2) we set:

$$x = \frac{S_b}{S_b^*}, \quad y = \frac{I_b}{I_b^*}, \quad z = \frac{A}{A^*}, \quad u = \frac{S_c}{S_c^*} \quad \text{and} \quad v = \frac{I_c}{I_c^*}.$$

Thus, system (2) is transformed into the following form:

$$
\begin{aligned}
\frac{dx}{dt} &= x\left[\frac{\Lambda_b}{S_b^*}\left(\frac{1}{x} - 1\right) - \beta_{bb}I_b^*(y - 1) - \beta_{bb}\epsilon A^*(z - 1) - \beta_{cb}I_c^*(v - 1)\right], \\[2mm]
\frac{dy}{dt} &= y\left[\beta_{bb}S_b^*(x - 1) + \frac{\beta_{bb}\epsilon A^* S_b^*}{I_b^*}\left(\frac{zx}{y} - 1\right) + \frac{\beta_{cb}I_c^* S_b^*}{I_b^*}\left(\frac{vx}{y} - 1\right)\right], \\[2mm]
\frac{du}{dt} &= u\left[\frac{\Lambda_c}{S_c^*}\left(\frac{1}{u} - 1\right) - \beta_{bc}I_b^*(y - 1) - \beta_{bc}\epsilon A^*(z - 1) - \beta_{cc}I_c^*(v - 1)\right], \\[2mm]
\frac{dv}{dt} &= v\left[\beta_{cc}S_c^*(u - 1) + \frac{\beta_{bc}\epsilon A^* S_c^*}{I_c^*}\left(\frac{zu}{v} - 1\right) + \frac{\beta_{bc}I_b^* S_c^*}{I_c^*}\left(\frac{yu}{v} - 1\right)\right], \\[2mm]
\frac{dz}{dt} &= z\left[\frac{f\gamma I_b^*}{A^*}\left(\frac{y}{z} - 1\right)\right].
\end{aligned}
\tag{6}
$$

It can easily be verified that model (6) has a unique endemic equilibrium $\mathcal{E}^*(1, 1, 1, 1, 1)$, and that the global stability of $\mathcal{E}^*$ is the same as that of system (2). Consider the Lyapunov function

$$
\begin{aligned}
\mathcal{U} &= S_b^*[x - 1 - \ln x] + I_b^*[y - 1 - \ln y] \\[2mm]
&\quad + \frac{[\beta_{bb}\epsilon A^* S_b^* + \beta_{bc}\epsilon A^* S_c^*]A^*}{f\gamma I_b^*}[z - 1 - \ln z] \\[2mm]
&\quad + S_c^*[u - 1 - \ln u] + I_c^*[v - 1 - \ln v].
\end{aligned}
$$

Differentiating $\mathcal{U}$ with respect to t along solutions of (6) gives:

$$
\begin{aligned}
\frac{d\mathcal{U}}{dt} &= +(x-1)\left[\Lambda_b\left(\frac{1}{x}-1\right)-\beta_{bb}I_b^*S_b^*(y-1)-\beta_{bb}\epsilon A^*S_b^*(z-1)-\beta_{cb}I_c^*S_b^*(v-1)\right] \\
&\quad +(y-1)\left[\beta_{bb}I_b^*S_b^*(x-1)+\beta_{bb}\epsilon A^*S_b^*\left(\frac{zx}{y}-1\right)+\beta_{cb}I_c^*S_b^*\left(\frac{vx}{y}-1\right)\right] \\
&\quad +(u-1)\left[\Lambda_c\left(\frac{1}{u}-1\right)-\beta_{bc}I_b^*S_c^*(y-1)-\beta_{bc}\epsilon A^*S_c^*(z-1)-\beta_{cc}I_c^*S_c^*(v-1)\right] \\
&\quad +(v-1)\left[\beta_{cc}I_c^*S_c^*(u-1)+\beta_{bc}\epsilon A^*S_c^*\left(\frac{zu}{v}-1\right)+\beta_{bc}I_b^*S_c^*\left(\frac{yu}{v}-1\right)\right] \\
&\quad +\frac{[\beta_{bb}\epsilon A^*S_b^*+\beta_{bc}\epsilon A^*S_c^*]}{f\gamma I_b^*}(z-1)\left[f\gamma I_b^*\left(\frac{y}{z}-1\right)\right] \\
&= F(x,y,z,u,v).
\end{aligned}
\tag{7}
$$

At endemic point we have the following identities:

$$
\begin{aligned}
\mu_b &= \frac{\Lambda_b}{S_b^*}-[\beta_{bb}I_b^*+\beta_{bb}\epsilon A^*+\beta_{cb}I_c^*], \\
(\mu_b+\gamma) &= \beta_{bb}S_b^*+\frac{\beta_{bb}\epsilon A^*S_b^*}{I_b^*}+\frac{\beta_{cb}I_c^*S_b^*}{I_b^*}, \\
(\sigma+\mu_c) &= \frac{\Lambda_c}{S_c^*}-[\beta_{bc}I_b^*+\beta_{bc}\epsilon A^*+\beta_{cc}I_c^*], \\
(\mu_c+d_c) &= \beta_{cc}S_c^*+\frac{\beta_{bc}\epsilon A^*S_c^*}{I_c^*}+\frac{\beta_{bc}I_b^*S_c^*}{I_c^*}, \\
(\mu_b+d_b) &= \frac{f\gamma I_b^*}{A^*}.
\end{aligned}
\tag{8}
$$

To assure that $F(x,y,z,u,v)\leq 0$ for $x>0, y>0, z>0, u>0, v>0$, the following condition must be satisfied $\beta_{cb}I_c^*S_b^*=\beta_{bc}(I_b^*+\epsilon A^*)S_c^*$ (see [34]). After some algebraic manipulations, we have

$$
\begin{aligned}
\frac{d\mathcal{U}}{dt} &= (\mu_bS_b^*+\beta_{bb}I_b^*S_b^*)\left(2-x-\frac{1}{x}\right)+\left((\sigma+\mu_c)S_c^*+\beta_{cc}I_c^*S_c^*\right)\left(2-u-\frac{1}{u}\right) \\
&\quad +\beta_{bb}\epsilon A^*S_b^*\left(3-\frac{1}{x}-\frac{y}{z}-\frac{zx}{y}\right)+\beta_{bc}I_b^*S_c^*\left(4-\frac{1}{x}-\frac{1}{u}-\frac{vx}{y}-\frac{yu}{v}\right) \\
&\quad +\beta_{bc}\epsilon A^*S_c^*\left(5-\frac{1}{x}-\frac{1}{u}-\frac{vx}{y}-\frac{zu}{v}-\frac{y}{z}\right).
\end{aligned}
$$

Since the arithmetic mean is greater or equal to the geometric mean, it can easily be verified that $\dot{\mathcal{U}}\leq 0$ provided that S_b^*, I_b^*, A^*, S_c^*, I_c^* are positive, where the equality $\dot{\mathcal{U}}=0$ holds only for $x=y=z=u=v=1$. Therefore $\dot{\mathcal{U}}\leq 0$ holds. Then the endemic equilibrium point Ω^* is globally asymptotically stable if $\mathcal{R}_0>1$ by LaSalle's invariance principle [32]. $\qquad\square$

2.1.3 Sensitivity analysis of the reproduction number

In this section we perform the sensitivity analysis of the model system (1). The threshold quantity $\mathcal{R}_0$ known as basic reproduction number is an important parameter to determine the persistence and extinction of brucellosis disease transmission in the population. To be able to suggest the most efficient way of controlling the disease we need to determine the parameters we can control and to

which $\mathcal{R}_0$ is more sensitive. Therefore we perform the sensitivity analysis of the model system (1) using partial rank correlated coefficient (PRCC) developed in [33] and the values of the parameters used in the model simulations are in Table (2) to demonstrate the influence of each parameter in the size of threshold quantity $\mathcal{R}_0$. PRCC is an efficient sensitivity analysis method based on sampling. PRCC assigns a value between -1 to $+1$ for each parameter. Positive PRCC value indicates a positive correlation of the parameter with the disease maintenance, whereas a negative value indicates a negative correlation with the infectiousness of the diseases. The Parameters studied are: Λ_b, Λ_c, Λ_h, μ_b, μ_c, μ_h, d_b, β_{bc}, β_{bb}, β_{cc}, β_{bh}, β_{ch}, f, θ, γ, σ, β_{bc}, d_c, ϵ.

Definition 2.1. (See, [33]) The normalized sensitivity index of $\mathcal{R}_0$ which depends on differentiability of parameter, ω is defined as follows:

$$\Psi_\omega^{\mathcal{R}_0} = \frac{\partial \mathcal{R}_0}{\partial \omega} \times \frac{\omega}{\mathcal{R}_0}. \tag{9}$$

From (9), the value of normalized sensitivity index for each parameter used in the model (1) is summarized in Table 1:

Table 1. Sensitivity analysis of parameters for the model system (1)

Parameter	Λ_b	Λ_c	Λ_h	μ_b	μ_c	μ_h	d_b
Index	+0.7399	+0.2601	0	-1.0476	-0.1141	0	-0.4615
Parameter	β_{bc}	β_{bb}	β_{cc}	β_{bh}	β_{ch}	f	θ
Index	+0.1937	+0.7399	0	0	0	+0.64	0
Parameter	γ	σ	β_{bc}	d_c	ϵ		
Index	-0.2308	-0.1460	+0.2601	0	+0.7691		
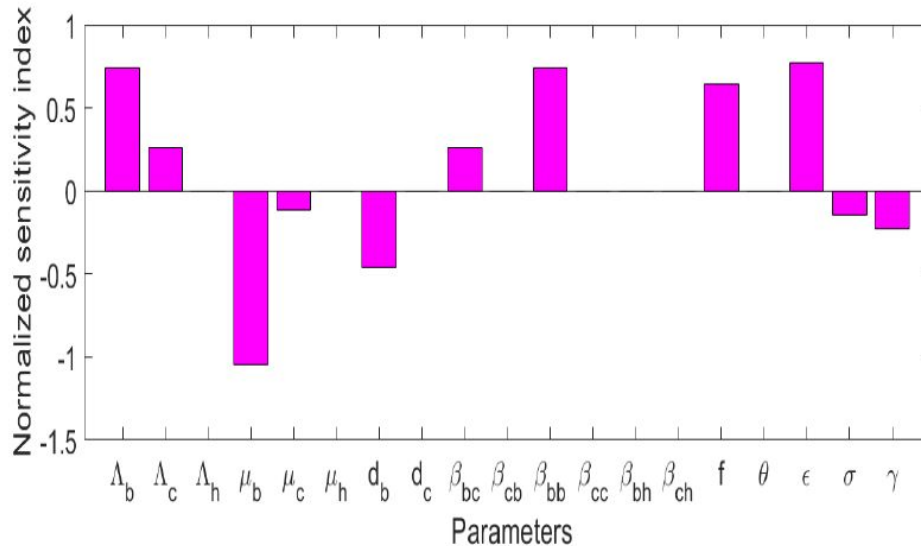
Fig. 2. Sensitivity analysis of the model system (1)

In Fig. 2, we observed that model parameters such as Λ_b, Λ_c, β_{bc}, β_{bb}, ϵ, and f, have a positive influence on the $\mathcal{R}_0$, that is, whenever they are increased, the size of $\mathcal{R}_0$ increases. For example, an increase in recruitment rate of Buffalo Λ_b by 73.99% will lead to an increase in the size of $\mathcal{R}_0$ by 73.99%. In the other-hand, model parameters with negative index values have a negative influence on $\mathcal{R}_0$, for example, an increase in mortality rate of Buffalo d_b by 46.15% will lead to a decrease on the magnitude of $\mathcal{R}_0$ by 46.15%.
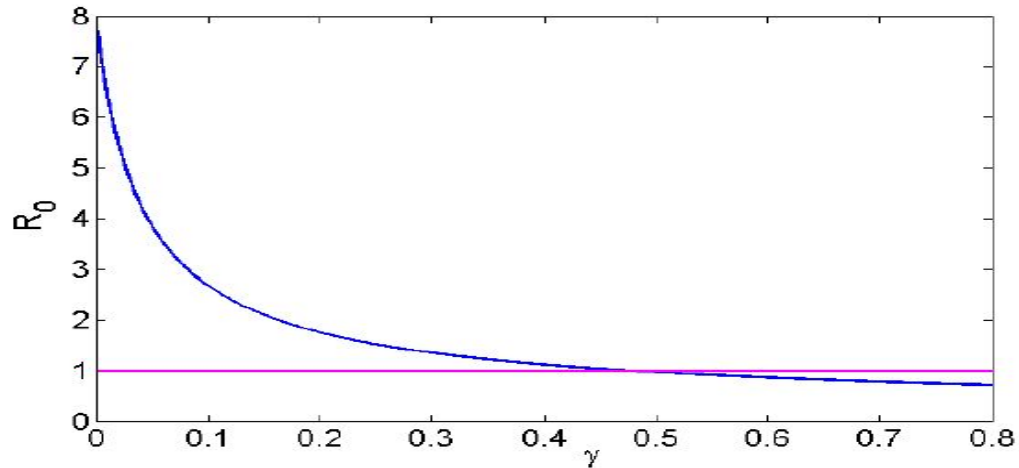
(a)
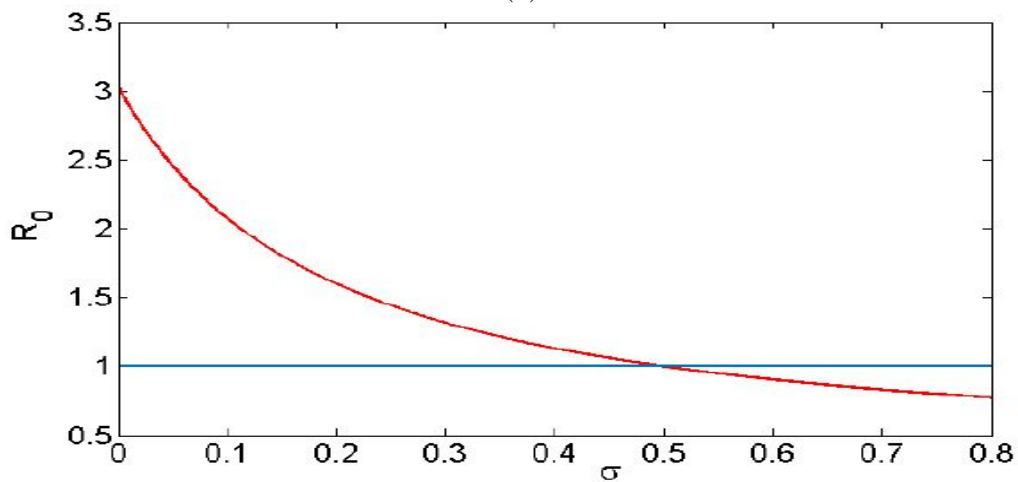
(b)

Fig. 3. Effects of varying (a) progression rate of infected cattle to chronic stage modeled by parameter γ on $\mathcal{R}_0$ (b) vaccination rate of susceptible cattle modeled by parameter σ on $\mathcal{R}_0$

Numerical results in Fig. 3a shows the progression rate of infected cattle from susceptible to chronic stage modeled by parameter γ on $\mathcal{R}_0$. Overall, we noted that increase on progression rate of infected cattle to chronic stage reduce the size of $\mathcal{R}_0$. In particular, one can note that whenever

the progression rate is greater than 0.5 the disease dies in the community. Fig 3b demonstrates the effect of vaccination rate of susceptible cattle on the spread of brucellosis disease in the population. Overall, we observed that whenever the vaccination rate of susceptible cattle is less than 0.5 the disease persists in the community.
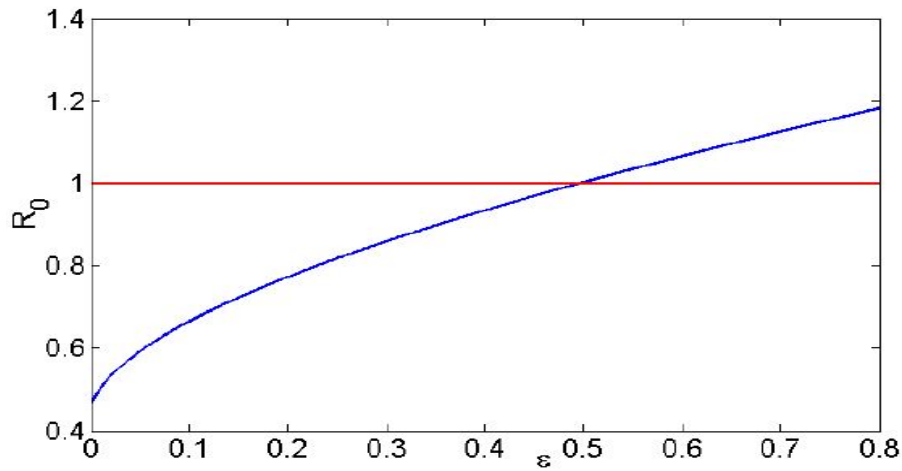

Fig. 4. Effects of varying rate of modifying factor for disease transmission modeled by parameter ϵ on $\mathcal{R}_0$

Fig.4 demonstrates the effects of modifying factor in the dynamics of brucellosis disease transmission. Overall, one can note that whenever the modifying factor for disease transmission is less then 0.5 the magnitude of $\mathcal{R}_0$ is less than unit and thus, the disease dies in the population.
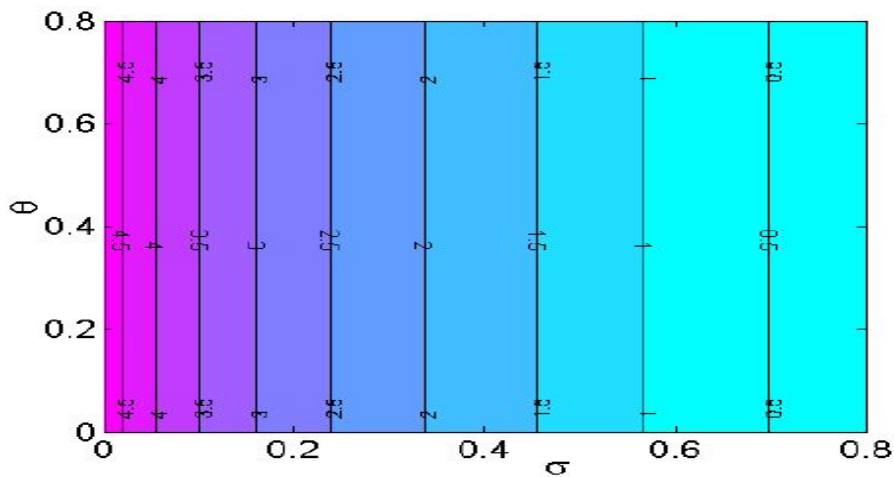

Fig. 5. Contour plot of the basic reproduction number $\mathcal{R}_0$ as the function of treatment rate of infected cattle (modeled by parameter θ) and vaccination rate of susceptible cattle (modeled by parameter σ)

Fig. 5 shows the contour plot of basic reproduction number $\mathcal{R}_0$ as the function of treatment rate of infected cattle (modeled by parameter θ) and vaccination rate of susceptible cattle (modeled by parameter σ). Overall, we noted that, increase on vaccination rate of susceptible and treatment of infected cattle reduce the size of $\mathcal{R}_0$. In particular one can note that whenever σ is greater than 0.5 the disease dies in the population.

2.2 A periodic brucellosis model

Infectious disease dynamics are often strongly influenced by seasonal patterns,irrespective of pathogen rate transmission mode [7, 35]. The breadth and consistency of these patterns suggest that seasonal influence on host and pathogen biology can have significant effects on patterns of pathogen invasion and transmission [36]. The relationship between host abundance and pathogen transmission, influenced strongly by seasons in some environments such as the semi-arid, is central to understanding infectious disease ecology and patterns and processes of pathogen invasion [7].

In fact, like many other infectious diseases, brucellosis is significantly influence by seasonal variations, and prior studies have demonstrated a strong connection between brucellosis infection and seasonal variations [7, 37, 38]. Factors such as the seasonal availability of forage which in turn lead to nomadic animal farming may be attributed to seasonality of brucellosis dynamics. Botswana provides an important example of this potential influence with extreme seasonal climatic variation, which occurs within and between years. In Botswana water availability is highly variable in time and space in relation to rainfall patterns and this can strongly influence density and spatial distribution of domestic animals and wildlife including buffalo over the whole year including buffalo calving periods [6].

Against this background, in this section, we extend model (1) to incorporate seasonality. Thus we introduce seasonal-induced transmission rate. Our new model takes the form:

$$
\left\{
\begin{array}{rcl}
\frac{dS_b}{dt} & = & \Lambda_b - [\beta_{bb}(t)(I_b + \epsilon A) + \beta_{cb}(t)I_c]S_b(t) - \mu_b S_b(t), \\
\frac{dI_b}{dt} & = & [\beta_{bb}(t)(I_b + \epsilon A) + \beta_{cb}(t)I_c]S_b(t) - [\mu_b + \gamma]I_b, \\
\frac{dA}{dt} & = & f\gamma I_b - [\mu_b + d_b]A(t), \\
\frac{dS_c}{dt} & = & \Lambda_c - [\beta_{bc}(t)(I_b + \epsilon A) + \beta_{cc}(t)I_c]S_c(t) - [\sigma + \mu_c]S_c(t), \\
\frac{dI_c}{dt} & = & [\beta_{bc}(t)(I_b + \epsilon A) + \beta_{cc}(t)I_c]S_c(t) - [\mu_c + d_c]I_c(t), \\
\frac{dS_h}{dt} & = & \Lambda_h - \beta_{bh}(t)(I_b + \epsilon A)S_h - \beta_{ch}(t)I_c S_h - \mu_h S_h + \theta I_h, \\
\frac{dI_h}{dt} & = & \beta_{bh}(t)(I_b + \epsilon A)S_h + \beta_{ch}(t)I_c S_h - (\theta + \mu_h)I_h.
\end{array}
\right.
\tag{10}
$$

All the variables and model parameters are assumed to be positive and they retain the same definitions as in model (1). Further, we assume that $\beta_{ij}(t)$, $(i, j = b, c, h)$ are periodic continuous functions in t with a period $\omega > 0$ (specifically, $\omega = 12$ months). Thus,

$$
\beta_{ij}(t) = \beta_{ij}\left[1 + a_k \sin\left(\frac{2\pi t}{12}\right)\right], \quad k = 1, 2, 3, 4, 5, 6
\tag{11}
$$

where β_{ij} denotes the basic contact rate without seasonal forcing and $0 < a_k < 1$ denotes the magnitude of seasonal fluctuations.

2.2.1 The reproductive number

To introduce the basic reproduction number in the fluctuating environment Wang and Zhao [39], extended the general procedure presented by Driessche and Watmough [30] by introducing the next infection operator

$$
(L\phi)(t) = \int_0^\infty Y(t, t - s)F(t - s)\phi(t - s)ds
\tag{12}
$$

Assume that $Y(t, s), t \geq s$, is the evolution operator of the linear ω-periodic system $\frac{dy}{dt} = V(t)y$ and $\phi(t)$, the initial distribution of infectious animals, is ω-periodic and always positive. Then effective reproductive number of the system (10) is then established by calculating the spectral radius of the next infection operator,

$$\mathcal{R}_s = \rho(L).$$

Thus, the evolution operator $Y(t, s)$, for the system (10) is

$$Y(t, s) = \begin{bmatrix} e^{-(\mu_b+\gamma)(t-s)} & 0 & 0 \\ \frac{f\gamma}{(\gamma-d_b)}[e^{-(\mu_b+d_b)(t-s)} - e^{-(\mu_b+\gamma)(t-s)}] & e^{-(\mu_b+d_b)(t-s)} & 0 \\ 0 & 0 & e^{-(\mu_c+d_c)(t-s)} \end{bmatrix}. \quad (13)$$

The next infection operator can be numerically evaluated by

$$(L\phi(t) = \int_0^\infty Y(t, t-s)F(t-s)\phi(t-s)ds = \int_0^T G(t, s)\phi(t-s)ds,$$

where

$$G(t, s) \quad \approx \quad \sum_{k=0}^M Y(t, t-s-k\omega)F(t-s)$$

$$\approx \quad \sum_{k=0}^M \begin{bmatrix} l_{11} & l_{12} & l_{13} \\ l_{21} & l_{22} & l_{23} \\ l_{31} & l_{32} & l_{33} \end{bmatrix},$$

for some positive integer M large enough, and

$$\begin{cases} \epsilon l_{11} & = & l_{12} = \epsilon \frac{\beta_{bb}(t-s)\Lambda_b}{\mu_b} e^{-(\mu_b+\gamma)(s+k\omega)}, \\[2mm] l_{13} & = & \frac{\beta_{cb}(t-s)\Lambda_b}{\mu_b} e^{-(\mu_b+\gamma)(s+k\omega)}, \\[2mm] \epsilon l_{21} & = & l_{22} = \epsilon \frac{f\gamma}{(\gamma-d_b)} \left[\frac{\beta_{bb}(t-s)\Lambda_b}{\mu_b} e^{-(\mu_b+d_b)(s+k\omega)} - l_{11} \right], \\[2mm] l_{23} & = & \left[\frac{\beta_{cb}(t-s)\Lambda_b}{\mu_b} e^{-(\mu_b+d_b)(s+k\omega)} - l_{13} \right], \\[2mm] \epsilon l_{31} & = & l_{32} = \epsilon \frac{\beta_{bc}(t-s)\Lambda_c}{(\sigma+\mu_c)} e^{-(\mu_c+d_c)(s+k\omega)}, \\[2mm] l_{33} & = & \frac{\beta_{cc}(t-s)\Lambda_c}{(\sigma+\mu_c)} e^{-(\mu_c+d_c)(s+k\omega)}. \end{cases}$$

In the special case of $\beta_{ij}(t) \equiv \beta_{ij}, \forall t \geq 0$, we obtain $F(t) \equiv F$, and $V(t) \equiv V, \forall t \geq 0$, then $\mathcal{R}_s = \mathcal{R}_0$.

2.2.2 Brucellosis extinction and persistence

In this section, we present that if $\mathcal{R}_s < 1$, then DFE is globally stable and the disease dies out. Then, if $\mathcal{R}_s > 1$ the disease persist.

In the special case of $\beta_{ij}(t) \equiv \beta_{ij}, \forall t \geq 0$, we obtain $F(t) \equiv F$, and $V(t) \equiv V, \forall t \geq 0$, then $\mathcal{R}_s = \mathcal{R}_0$. It can easily be verified that system (10) satisfies assumptions (A1)-(A7) in Wang and Zhao (2008) [39]. Thus, we have the following results , which are crucial for our simulations and the main analytical results in this section.

Lemma 2.3. *(Wang and Zhao Theorem 2.2 in [39]). The following statements are valid:*

(i) $\mathcal{R}_0 = 1$ *if and only if* $\rho(\Phi_{(F-V)}(\omega)) = 1$.

(ii) $\mathcal{R}_0 > 1$ *if and only if* $\rho(\Phi_{(F-V)}(\omega)) > 1$.

(ii) $\mathcal{R}_0 < 1$ *if and only if* $\rho(\Phi_{(F-V)}(\omega)) < 1$.

We now proceed to prove Theorem 2.5.

Proof. In the case where $\mathcal{R}_s < 1$, Lemma 2.3 implies that $\mathcal{E}^0$ is locally asymptotically stable. It suffices to prove that $\mathcal{E}^0$ is globally attractive in Γ.

Assume that $\mathcal{R}_s < 1$, By Lemma 2.3, it follows that for any $\varphi > 0$, there exists large $t_0 > 0$ such that $S_b(t) < S_b^0 + \varphi$ and $S_c < S_c^0 + \varphi$, when $t > t_0$. Then for system (10), we have, when $t > t_0$, that

$$\begin{cases} \dot{I}_b(t) & \leq & [\beta_{bb}(t)(I_b + \epsilon A) + \beta_{cb}(t)I_c][S_b^0(t) + \varphi] - [\mu_b + \gamma]I_b, \\ \dot{A}(t) & = & f\gamma I_b - [\mu_b + d_b]A(t), \\ \dot{I}_c(t) & \leq & [\beta_{bc}(t)(I_b + \epsilon A) + \beta_{cc}(t)I_c][S_c^0(t) + \varphi] - [\mu_c + d_c]I_c(t). \end{cases} \tag{14}$$

Considering the comparison system,

$$\frac{dh}{dt} = (F(t) - V(t) + M_\varphi)h(t), \quad h(t) = (I_b(t), I_c(t), A(t)). \tag{15}$$

By Lemma 2.1 in [40], it follows that there exists a positive ω-periodic function $\bar{h}(t)$ such that $h(t) = e^{\psi t}\bar{h}(t)$ is a solution of the system (15) where $\psi = \frac{1}{\omega}\ln\rho(\Phi_{(F-V+M_\varphi)(\cdot)}(\omega))$. Further, we know that $\mathcal{R}_s < 1$, if and only if $\rho(\Phi_{(F-V+M_\varphi)(\cdot)}(\omega)) < 1$. Since $\rho(\Phi_{(F-V+M_\varphi)(\cdot)}(\omega)) < 1$, it follows that, ψ is a negative constant. Therefore, we have $h(t) \longrightarrow 0$ as $t \longrightarrow +\infty$. This implies that the zero solution of system (15) is globally asymptotically stable. For any non-negative initial value $(I_b(0), A(0), I_c(0)))^T$ for system (14), there a sufficient large $M^* > 0$ such that $(I_b(0), A(0), I_c(0))^T \leq M^*\bar{h}(0)$ holds. Following the comparison principle [41], we have $(I_b(t), A(t), I_c(t))^T \leq M^*h(t)$ for all $t > 0$ where $M^*h(t)$ is also a solution of system (15). Therefore, we get $I_b(t) \longrightarrow 0$, $A(t) \longrightarrow 0$ and $I_c(t) \longrightarrow 0$, as $t \longrightarrow +\infty$. By the theory of asymptotic autonomous systems [42], it then follows that $S_b(t) \longrightarrow S_b^0$ and $S_c(t) \longrightarrow S_c^0$. So $\mathcal{E}^0$ is globally attractive when $\mathcal{R}_s < 1$. It follows that $\mathcal{E}^0$ is globally asymptotically stable when $\mathcal{R}_s < 1$. □

Define:

$$X_0 = \{(S_b, S_c, A, I_b, I_c) \in \mathbb{R}_+^5 : A > 0, I_b > 0, I_c > 0\}. \qquad \partial X_0 = \mathbb{R}_+^5 \backslash X_0.$$

Let $P : \mathbb{R}_+^5 \longrightarrow \mathbb{R}_+^5$ be the Poincaré map associated with system (10) such that

$$P(x_0) = u(\omega, x_0), \quad \forall x_0 \in \mathbb{R}_+^5,$$

where $u(t, x_0)$ denotes the unique solution of the system (10) with $u(0, x_0) = x_0$. It is easy to verify that

$$P^m(x_0) = u(m\omega, x_0), \quad \forall_m > 0,$$

Lemma 2.4. *When* $\mathcal{R}_s > 1$, *then there exists a* $\delta > 0$ *such that when*

$$\|(S_b^0, I_b^0, A^0, S_c^0, I_c^0) - P_0\| \leq \delta$$

for any $(S_b^0, I_b^0, A^0, S_c^0, I_c^0) \in X_0$, *we have*

$$\limsup_{m \to \infty} d[P^m(S_b^0, I_b^0, A^0, S_c^0, I_c^0), P_0] \geq \delta \tag{16}$$

where $P_0 = (S_b^0, 0, 0, S_c^0, 0)$.

Proof. If $\mathcal{R}_0 > 1$, we obtain $\rho(\Phi_{(F-V)}(\omega)) > 1$ by Lemma 2.3. Choose $\tilde{\epsilon}$ small enough such that $\rho(\Phi_{(F-V-M_{\tilde{\epsilon}})}(\omega)) > 1$, where

$$M_{\tilde{\epsilon}} = \begin{bmatrix} \tilde{\epsilon} & \tilde{\epsilon} & \tilde{\epsilon} \\ \tilde{\epsilon} & \tilde{\epsilon} & \tilde{\epsilon} \\ 0 & 0 & 0 \end{bmatrix}.$$

Now we proceed by contradiction to prove that

$$\limsup_{m \to \infty} d[P^m(S_b^0, I_b^0, A^0, S_c^0, I_c^0), P_0] \geq \delta.$$

If not, then

$$\limsup_{m \to \infty} d[P^m(S_b^0, I_b^0, A^0, S_c^0, I_c^0), P_0] < \delta,$$

for some $(S_b^0, I_b^0, A^0, S_c^0, I_c^0) \in X_0$. Without loss of generality, we assume that $d[P^m(S_b^0, I_b^0, A^0, S_c^0, I_c^0), P_0] < \delta$ for all $m \geq 0$. By the continuity of the solution with respect to the initial values, we obtain

$$\|u(t, P^m(S_b^0, I_b^0, A^0, S_c^0, I_c^0)) - u(t_1, P_0)\| \leq \tilde{\epsilon}, \quad \forall m \geq 0, \quad \forall t_1 \in [0, \omega].$$

For any $t \geq 0$, let $t = m\omega + t_1$, where $t_1 \in [0, \omega]$ and $m = [\frac{t}{\omega}]$, which the greatest integer less than or equal to $\frac{t}{\omega}$. Then we have

$$\|u(t, (S_b^0, I_b^0, A^0, S_c^0, I_c^0)) - u(t, P_0)\| = \|u(t_1, P^m(S_b^0, I_b^0, A^0, S_c^0, I_c^0)) - u(t_1, P_0)\| \leq \tilde{\epsilon}$$

for any $t \geq 0$, which implies that $S_b^0 - \tilde{\epsilon} < S_b(t) < S_b^0 + \tilde{\epsilon}$, $S_c^0 - \tilde{\epsilon} < S_c(t) < S_c^0 + \tilde{\epsilon}$, $t \geq 0$. Then for $\|(S_b^0, I_b^0, A^0, S_c^0, I_c^0) - P_0\| \leq \delta$, we have

$$\begin{cases} \dot{I}_b(t) & \geq & [\beta_{bb}(t)(I_b + \epsilon A) + \beta_{cb}(t)I_c][S_b^0(t) - \tilde{\epsilon}] - [\mu_b + \gamma]I_b, \\ \dot{A}(t) & = & f\gamma I_b - [\mu_b + d_b]A(t), \\ \dot{I}_c(t) & \geq & [\beta_{bc}(t)(I_b + \epsilon A) + \beta_{cc}(t)I_c][S_c^0(t) - \tilde{\epsilon}] - [\mu_c + d_c]I_c(t). \end{cases} \quad (17)$$

Next we consider the linear system

$$\begin{cases} \dot{I}_b(t) & = & [\beta_{bb}(t)(I_b + \epsilon A) + \beta_{cb}(t)I_c][S_b^0(t) - \tilde{\epsilon}] - [\mu_b + \gamma]I_b, \\ \dot{A}(t) & = & f\gamma I_b - [\mu_b + d_b]A(t), \\ \dot{I}_c(t) & = & [\beta_{bc}(t)(I_b + \epsilon A) + \beta_{cc}(t)I_c][S_c^0(t) - \tilde{\epsilon}] - [\mu_c + d_c]I_c. \end{cases} \quad (18)$$

Once again by Lemma 2.3, it follows that there exists a positive $\omega-$ periodic function $\tilde{g}(t)$ such that $g(t) = e^{pt}\tilde{g}(t)$ is a solution of system (18), where $p = \frac{1}{\omega} \ln \rho(\Phi_{F-V-M_{\tilde{\epsilon}}}(\omega))$. Because $\rho(\Phi_{F-V-M_{\tilde{\epsilon}}}(\omega)) > 1$, when $g(0) > 0$, $g(t) \to \infty$ as $t \to$. Applying the comparison principle [41], we know that when $I_b(0) > 0$, $A(0) > 0$ and $I_c(0) > 0$, $I_b(t) \to \infty$, $A(t) \to \infty$ and $I_c(t) \to \infty$ as $t \to \infty$. This is a contradiction. This completes the proof. □

Theorem 2.5. *If the basic reproduction number $\mathcal{R}_s < 1$, then the unique DFE is globally asymptotically stable in Γ. Further, if $\mathcal{R}_s > 1$ the disease persists.*

2.3 Optimal control

In this section, we turn to an optimal control study of our brucellosis models, with an aim of exploring effective prevention and intervention strategies that could best balance the outcomes and costs of the control. To that end, we will perform the optimal control study both the autonomous model (1) and non-autonomous model (10). We introduce two time-dependent control strategies, $u_1(t)$ and $u_2(t)$ which are represented as functions of time and assigned reasonable upper and lower bounds. The control function $u_1(t)$ measures the rate at which susceptible cattle are vaccinated

during each time period, while control function $u_2(t)$ accounts for the impact of detection and culling of infectious cattle. Since humans do not transmit the disease we did not consider time dependent intervention strategy. Retaining the same variable and parameter names as in (1), the system of differential equations describing our model with controls is:

$$
\begin{cases}
\frac{dS_b}{dt} &= \Lambda_b - [\beta_{bb}(I_b + \epsilon A) + \beta_{cb}I_c]S_b - \mu_b S_b, \\
\frac{dI_b}{dt} &= [\beta_{bb}(I_b + \epsilon A) + \beta_{cb}I_c]S_b - [\mu_b + \gamma]I_b, \\
\frac{dA}{dt} &= f\gamma I_b - [\mu_b + d_b]A, \\
\frac{dS_c}{dt} &= \Lambda_c - [\beta_{bc}(I_b + \epsilon A) + \beta_{cc}I_c]S_c - [\sigma u_1(t) + \mu_c]S_c, \\
\frac{dI_c}{dt} &= [\beta_{bc}(t)(I_b + \epsilon A) + \beta_{cc}I_c]S_c - [\mu_c + \alpha u_2(t) + \delta]I_c, \\
\frac{dS_h}{dt} &= \Lambda_h - \beta_{bh}(I_b + \epsilon A)S_h - \beta_{ch}I_c S_h - \mu_h S_h + \theta I_h, \\
\frac{dI_h}{dt} &= \beta_{bh}(I_b + \epsilon A)S_h + \beta_{ch}I_c S_h - (\theta + \mu_h)I_h.
\end{cases}
\tag{19}
$$

According to the extended model above, an optimal control problem with the objective function is formulated by

$$
\text{Minimize} \quad J\Big(u_1(t), u_2(t)\Big) = \int_0^T \left[BI_c(t) + \frac{W_1}{2}u_1^2(t) + \frac{W_2}{2}u_2^2(t) \right] dt.
\tag{20}
$$

The objective is to minimize infected cattle population over a finite time interval $[0, T]$ at minimal costs. In equation (20), B_1 represent weight constant of the infected cattle. In addition, W_1 and W_2 are weight for cattle vaccination and cattle culling. The control efforts in equation (20) are assumed to be nonlinear-quadratic, since a quadratic structure in the control has mathematical advantages, such as: if the control set is compact and convex it follows that the Hamiltonian attains its minimum over the control set at a unique point [43, 44, 45, 46, 47, 48]. Further, $W_1 u_1^2(t)$, and $W_2 u_2^2(t)$ describe the costs associated with vaccination and culling, respectively. We assumed that the costs are proportional to the square of the corresponding control function.
The control set is defined as

$$
\Omega = \Big\{ (u_1(t), u_2(t)) \,\big|\, 1 \le u_1(t) \le U_1, 1 \le u_2(t) \le U_2 \},
\tag{21}
$$

where U_1, and U_2 denote the upper bounds for the efforts of vaccination, culling and human treatment, respectively. The bounds reflect practical limitation on the maximum rate of control that can be implemented in a given time period. If, however, $u_1(t) = u_2(t) = 1$ for all t, then the model (19) is reduced to the original model (1) or (10), with regular (i.e., minimum) controls.
The optimal control problem hence becomes that we seek optimal functions, $(u_1^*(t), u_2^*(t))$, such that

$$
J\Big(u_1^*(t), u_2^*(t)\Big) = \min_\Omega J\Big(u_1(t), u_2(t)\Big)
\tag{22}
$$

subject to the state equations in system (19) with initial conditions. The existence of optimal control follows from standard results in optimal control theory [48, 49]. The necessary conditions that optimal controls must satisfy are derived using Pontryagin's Maximum Principle [50]. Thus, system (2) is converted into an equivalent problem, namely the problem of minimizing the Hamiltonian H

given by:

$$
\begin{aligned}
H(t) &= BI_c(t) + \frac{W_1}{2}u_1^2(t) + \frac{W_2}{2}u_2^2(t) \\
&\quad + \lambda_{S_b}(t)\Big[\Lambda_b - (\beta_{bb}(I_b + \epsilon A) + \beta_{cb}I_c)S_b - \mu_b S_b\Big] \\
&\quad + \lambda_{I_b}(t)\Big[(\beta_{bb}(I_b + \epsilon A) + \beta_{cb}I_c)S_b - (\mu_b + \gamma)I_b\Big] \\
&\quad + \lambda_A(t)\Big[f\gamma I_b - (\mu_b + d_b)A\Big] \\
&\quad + \lambda_{S_c}(t)\Big[\Lambda_c - (\beta_{bc}(I_b + \epsilon A) + \beta_{cc}I_c)S_c - (\sigma u_1(t) + \mu_c)S_c\Big] \\
&\quad + \lambda_{I_c}(t)\Big[(\beta_{bc}u_2(t)(I_b + \epsilon A) + \beta_{cc}I_c)S_c - (\mu_c + \alpha u_2(t) + \delta)I_c\Big] \\
&\quad + \lambda_{S_h}(t)\Big[\Lambda_h - \beta_{bh}(I_b + \epsilon A)S_h - \beta_{ch}I_c S_h - \mu_h S_h + \theta I_h\Big] \\
&\quad + \lambda_{I_h}(t)\Big[\beta_{bh}(I_b + \epsilon A)S_h + \beta_{ch}I_c S_h - (\theta + \mu_h)I_h\Big],
\end{aligned}
$$

where $\lambda_{S_b}(t)$, $\lambda_{I_b}(t)$, $\lambda_A(t)$, $\lambda_{S_c}(t)$, $\lambda_{I_c}(t)$, $\lambda_{S_h}(t)$ and $\lambda_{I_h}(t)$ denote the adjoint functions associated with the states S_b, I_b, A, S_c and I_c, respectively. Note that, in $H(t)$, each adjoint function multiplies the right-hand side of the differential equation of its corresponding state function. The first term in $H(t)$ comes from the integrand of the objective functional.

Given an optimal control treble (u_1^*, u_2^*, u_3^*) and corresponding states (S_b, I_b, A, Sc, I_c), there exist adjoint functions [?] satisfying

$$
\frac{d\lambda_{S_b}(t)}{dt} = -\frac{\partial H}{\partial S_b}, \ \frac{d\lambda_{I_b}(t)}{dt} = -\frac{\partial H}{\partial I_b}, \ \frac{d\lambda_A(t)}{dt} = -\frac{\partial H}{\partial A},
$$

$$
\frac{d\lambda_{S_c}(t)}{dt} = -\frac{\partial H}{\partial S_c}, \ \frac{d\lambda_{I_c}(t)}{dt} = -\frac{\partial H}{\partial I_c}, \ \frac{d\lambda_{S_h}(t)}{dt} = -\frac{\partial H}{\partial S_h}, \ \frac{d\lambda_{I_h}(t)}{dt} = -\frac{\partial H}{\partial I_h}. \tag{23}
$$

These yield

$$
\begin{aligned}
\frac{d\lambda_{S_b}(t)}{dt} &= \lambda_{S_b}(t)\Big(\beta_{bb}(I_b + \epsilon A) + \beta_{cb}I_c + \mu_b\Big) - \lambda_{I_b}(t)\Big(\beta_{bb}(I_b + \epsilon A) + \beta_{cb}I_c\Big), \\
\frac{d\lambda_{I_b}(t)}{dt} &= \lambda_{S_b}\beta_{bb}S_b + \lambda_{I_b}(t)\Big(\mu_b + \gamma - \beta_{bb}S_b\Big) - f\gamma\lambda_A(t) + \lambda_{S_c}(t)\beta_{bc}(t)S_c - \lambda_{I_c}(t)\beta_{bc}(t)S_c \\
&\quad + \lambda_{S_h}(t)\beta_{bh}S_h - \lambda_{I_h}(t)\beta_{bh}S_h, \\
\frac{d\lambda_A(t)}{dt} &= \lambda_{S_b}(t)\beta_{bb}\epsilon S_b + \lambda_{S_c}(t)\beta_{bc}\epsilon S_c - \lambda_{I_c}(t)\beta_{bc}\epsilon S_c - \lambda_{I_b}(t)\beta_{bb}\epsilon S_b + \lambda_A(\mu_b + d_b), \\
&\quad + \lambda_{S_h}\beta_{bh}\epsilon S_h - \lambda_{I_h}\beta_{bh}\epsilon S_h, \\
\frac{d\lambda_{S_c}(t)}{dt} &= \lambda_{S_c}(t)\Big(\beta_{bc}(I_b + \epsilon A) + \beta_{cc}I_c + \mu_c + \sigma u_1(t)(t)\Big) - \lambda_{I_b}(t)\Big(\beta_{bc}(I_b + \epsilon A) + \beta_{cc}I_c\Big), \\
\frac{d\lambda_{I_c}(t)}{dt} &= -B + \lambda_{S_b}(t)\beta_{cb}S_b - \lambda_{I_b}(t)\beta_{cb}S_b + \lambda_{S_c}(t)\beta_{cc}S_c + \lambda_{I_c}(t)\Big(\mu_c + \alpha u_2(t) + \delta - \beta_{cc}S_c\Big) \\
&\quad + \lambda_{S_h}\beta_{ch}S_h - \lambda_{I_h}\beta_{ch}S_h, \\
\frac{d\lambda_{S_h}(t)}{dt} &= \lambda_{S_h}(\beta bh(I_b + \epsilon A) + \beta_{ch}I_c + \mu_h) - \lambda_{I_h}(\beta bh(I_b + \epsilon A) + \beta_{ch}I_c), \\
\frac{d\lambda_{I_h}(t)}{dt} &= \lambda_{I_h}(t)(\theta + \mu_h) - \lambda_{S_h}(t)\theta,
\end{aligned}
$$

with transversality conditions $\lambda_i(T) = 0$, for $i = S_b(t), I_b(t), A(t), S_c(t), I_c(t), S_h(t), I_h(t)$. Furthermore, the optimal controls are characterized by the optimality conditions:

$$
u_1^*(t) = \max[1, \min(\bar{u}_1(t), U_1)], \qquad u_2^*(t) = \max[1, \min(\bar{u}_2(t), U_2)]. \tag{24}
$$

where

$$\bar{u}_1(t) = \frac{\sigma S_c \lambda_{S_c}}{2W_1}, \qquad \bar{u}_2(t) = \frac{\alpha I_c \lambda_{I_c}}{2W_2}. \tag{25}$$

While it is known that wildlife can be important in brucellosis transmission dynamics, lack of data present an enormous challenge to modellers on evaluating animal and public health control strategies. Wildlife present a complex component of transmission that can be difficult to characterize and there is a need for surveillance data to be coupled with molecular, genetic, and dynamical modeling tools in order to begin to unravel this complexity [7]. Despite the unavailability of surveillance data we proceed to explore the numerical solutions to our autonomous model. Parameter values and variables used in our simulations are listed in Table 2.

In the formulation above, the parameters β_{ij}, $(i, j = b, c, h)$ can be either constants, for the autonomous model (1), or periodic functions in the form of equation (11), for the periodic model (10). For each case, the state equations, adjoint equations and optimality conditions constitute an optimal control problem, which is then solved numerically.

We adopted the following initial population levels from [13], $S_c(0) = 1.33 \times 10^6$, $I_c(0) = 3.3 \times 10^5$, $S_h(0) = 1.618 \times 10^6$, $I_h = 0$ and estimate the African buffalo population levels as follows $S_b(0) = 4.341 \times 10^7$, $I_b(0) = 1.33 \times 10^6$ and $A(0) = 0$. For simplicity we set $B = 1$. We further assume that vaccination incurs higher costs than those for culling so that $W_1 > W_2$. More specifically we set $W_1 = 10^6$ and $W_2 = 10^3$. In addition, we set the control bound of $u_1(t)$ and $u_2(t)$ as follows $U_1 = 20$ and $U_2 = 3$, respectively.

Baseline values for our model parameter have been adopted from various source abound in literature as indicated in Table 2. Since prior studies suggests that the optimal treatment of uncomplicated brucellosis should be based on a six-week regimen of doxycycline combined either with streptomycin for 2–3 weeks, or rifampicin for six weeks [29], we assume that the average treatment duration is 4 weeks and then $\theta = \frac{52}{4} = 13$.

Table 2. Parameters and values

Symbol	Definition	Value	Units	Source
$(\Lambda_b, \Lambda_c, \Lambda_h)$	Recruitment rate	(1680000,1976000,9150)	year^{-1}	[13]
(μ_b, μ_c, μ_h)	Natural elimination rate	(0.04,0.22,0.02)	year^{-1}	[12, 51]
(d_b, d_c)	Disease-related death rate	(0.35, 0.2)	year^{-1}	[12]
$a_k(k = 1, 2, 3, 4)$	Amplitude of oscillation	0.8		
(β_{bc}, β_{cb})	Averaged direct transmission rate	0.135×10^{-6}	animal^{-1}year^{-1}	[13]
β_{bb}	Averaged direct transmission rate	0.21×10^{-6}	animal^{-1}year^{-1}	[13]
β_{cc}	Averaged direct transmission rate	0.18×10^{-6}	animal^{-1}year^{-1}	[13]
β_{bh}	Averaged direct transmission rate	1.3458×10^{-9}	animal^{-1}year^{-1}	[13]
β_{ch}	Averaged direct transmission rate	0.5896×10^{-9}	animal^{-1}year^{-1}	[13]
f	Proportion of new infections that develop into chronic	0.8		[11]
γ	Rate of progression to chronic carrier state African buffaloes	0.67	year^{-1}	[51]
θ	Human treatment rate	13	year^{-1}	[29]
ϵ	Modification factor	0.5		
σ	Vaccination rate	0.316	year^{-1}	[11]

Fig. 6 depict the numbers of infected wildlife, cattle and human over finite time interval in the presence and absence of optimal control. The results demonstrate that optimal control strategy a significant effect on the numbers of infected wildlife, cattle and humans, though, these control strategies are targeting cattle population only. Similar behavior is also present on the results for the periodic model (see Fig. 7, but with oscillatory patterns indicate the influence of seasonality on brucellosis dynamics. Results in both Fig. 6 and Fig. 7 shows that the implementation of time dependent intervention strategies aimed targeting domesticated livestock may not be sufficient to
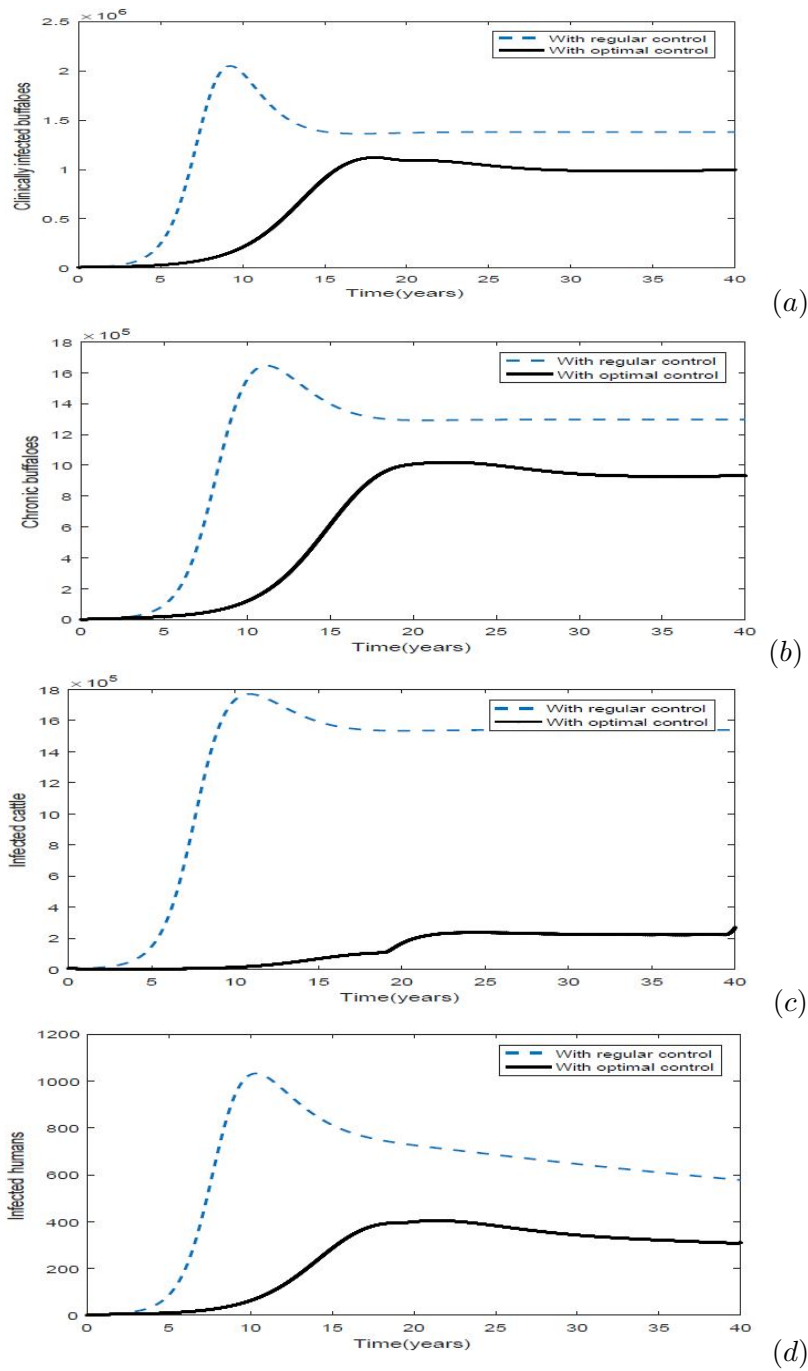
Fig. 6. The numbers of infected wildlife, cattle and human for the autonomous model (1): (*a*) **clinically infected buffaloes** (*b*) **chronically infected buffaloes;** (*c*) **infected cattle;** (*d*) **infected humans.**
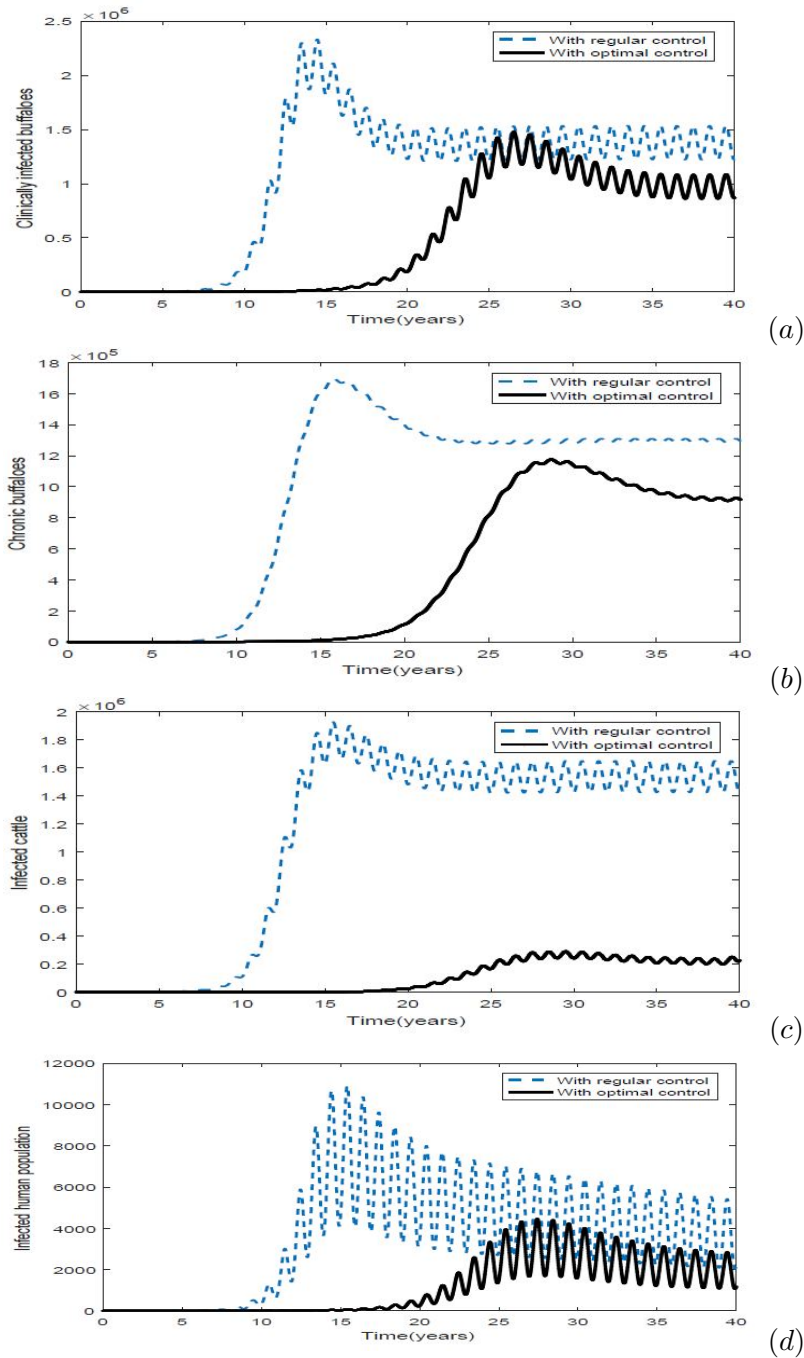
Fig. 7. The numbers of infected wildlife, cattle and human for the periodic model (10): (*a*) **clinically infected buffaloes** (*b*) **chronically infected buffaloes;** (*c*) **infected cattle;** (*d*) **infected humans.**
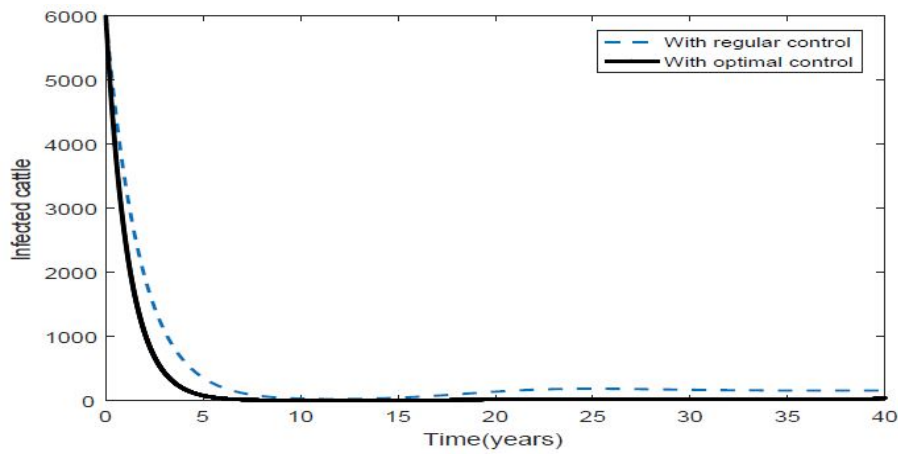
Fig. 8. The numbers of infected cattle for the autonomous model (1) with extremely minimal interaction between wildlife and both cattle and humans.
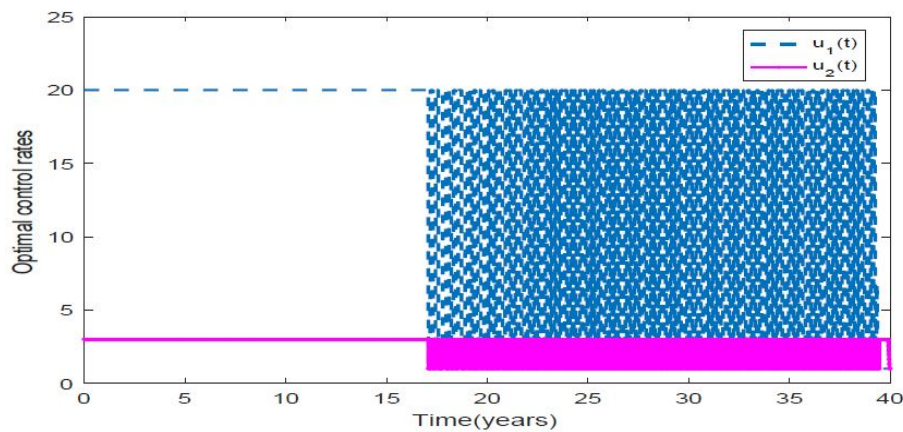

Fig. 9. Control profiles for the periodic model (10)

control the spread of human brucellosis in communities where cattle, wildlife and human interact. However, when there is extremely minimum interaction between wildlife and both cattle and humans (we set $\beta_{cb} = \beta_{bc} = 0.21 \times 10^{-10}$) we observe that optimal vaccination and culling of cattle will lead to brucellosis elimination (see Fig. 8).

Fig. 9 depicts the optimal control profiles for $u_1(t)$ and $u_2(t)$ for the periodic model (10). As we can observe, both u_1 and u_2 starts at the maximum and remain there for a period of 18 years. There after both controls (u_1 and u_2) begin to oscillate with time for all the remaining period. These results suggest a maximum effort for vaccination and culling for the entire horizon. A similar remark can be drawn for an autonomous model (1) since both controls u_1 and u_2 start at the maximum and remain there for the entire time horizon see Fig. 10.

To explore the effects of costs on the implementation of control strategies, we varied W_1 and W_2. Suppose $W_1 = 10^{10}$ and $W_2 = 10^5$. Then as illustrated in Fig. 11 control u_1 and u_2 will not stay
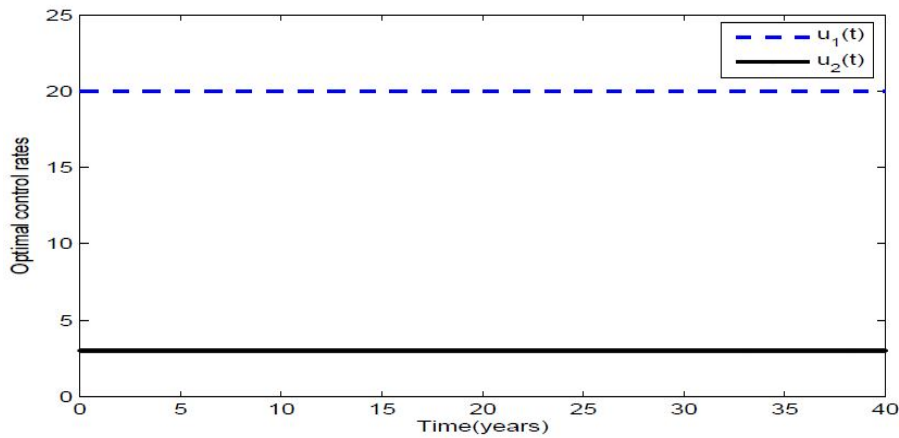
Fig. 10. Control profiles for the periodic model (1)

at the maximum for the entire time horizon as we have observed earlier. More specifically, u_1 will stay at the maximum for a period of 2 years while u_2 will stay at the maximum for about 7 years and this is due to the relatively lower value of W_2.
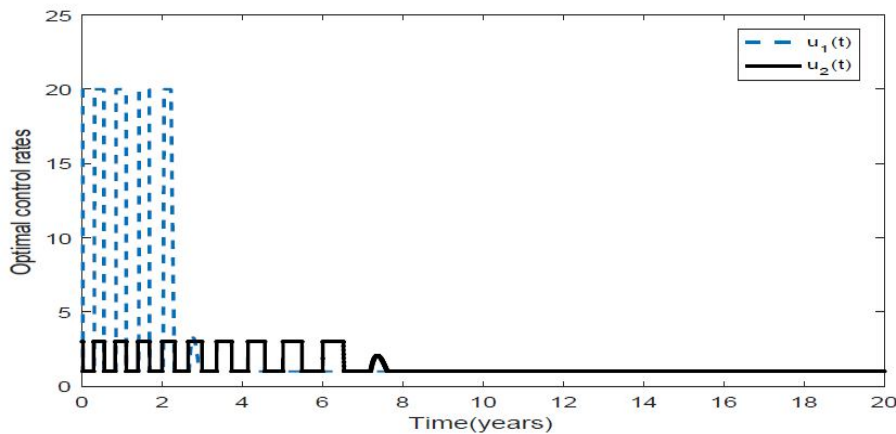

Fig. 11. Control profiles for the periodic model (10) with high costs

3 Concluding Remarks

In this paper, we constructed a theoretical framework to investigate the transmission dynamics of human brucellosis in periodic and non-periodic environments. We also investigated the implications of intervention strategies on controlling the spread of brucellosis. To explore brucellosis dynamics in non-periodic environments we developed an autonomous dynamical system with constant parameters that account for all the essential biological dynamics of brucellosis. Our model incorporated human population, cattle population and wildlife population (African buffaloes). We conducted thorough analysis of the model, including computation of the basic reproduction number and stability analysis of the model steady states. Particularly, we demonstrated that when the basic reproduction number

is less than unity then our autonomous model has globally stable disease free equilibrium. This implies that the disease dies out in the community. However, if the basic reproduction number is greater than unity then there exists a unique endemic equilibrium that is globally asymptotically stable.

Extensive investigation of the relationship between reproduction number $\mathcal{R}_0$ and model parameters, we observed that model parameters such as Λ_b, Λ_c, β_{bc}, β_{bb}, ϵ, and f, have a positive influence on the $\mathcal{R}_0$, that is, whenever they are increased, the size of $\mathcal{R}_0$ increases. For example, an increase in recruitment rate of Buffalo Λ_b by 73.99% will lead to an increase in the size of $\mathcal{R}_0$ by 73.99%. In the other-hand, model parameters with negative index values have a negative influence on $\mathcal{R}_0$, for example, an increase in mortality rate of Buffalo d_b by 46.15% will lead to a decrease on the magnitude of $\mathcal{R}_0$ by 46.15%. Overall, we noted that increase on progression rate of infected cattle to chronic stage reduce the size of $\mathcal{R}_0$. In particular, one can note that whenever the progression rate is greater than 0.5 the disease dies in the community. Furthermore, we observed that whenever the vaccination rate of susceptible cattle is less than 0.5 the disease persists in the community.

The model allowed us to demonstrate the implications of time dependent controls. Specifically we have shown that time dependent intervention strategies for cattle population could minimized brucellosis incidence in both humans and wildlife. In addition, our optimal control simulations demonstrate that if humans and cattle have extremely minimal interaction then brucellosis can be effectively controlled in both humans and cattle and it may require a period of 5 years to successful contain the disease. However, if the intervention strategies are regular the disease may not be successful contained even if the strategies are implemented for a time period of 40 years.

In the second model, we extended the autonomous system to a periodic environment to analyze the impacts of seasonal variation that may affect the movements of animals and, consequently, brucellosis transmission. We derived an expression for the seasonal-induced basic reproductive number and showed that the basic reproductive number remains a sharp threshold for brucellosis dynamics even in a periodic environment. Thus, if the basic reproduction number is less than unity brucellosis will be eradicated. We also proved uniform persistence of the disease as well as the existence of a nontrivial periodic solution when the basic reproduction number is greater than unity. In a similar manner, to our autonomous model, we explored the implication of time dependent cattle vaccination and culling of infected cattle. Our optimal control simulations in this case concurred with our earlier findings on the autonomous model, that optimal control can greatly reduce brucellosis incidence among human, wildlife and cattle. However, our optimal control simulations of the periodic model also exhibited annual oscillations which reflect the effect of seasonality on brucellosis dynamics in periodic environments. In conclusion, our study demonstrate that, in all scenarios, the optimal control can greatly reduce the burden of brucellosis in the community and most importantly if wildlife and cattle and humans and cattle have extremely minimal contacts then the disease can be effectively controlled in a shorter period of time.

A potential limitation of the present paper is that we have employed the mass action incidence for the direct transmission route for both the autonomous and time-periodic model. Such mass action forms, with the advantage of making model calculations more tractable, have been extensively used in previously published brucellosis modeling work (see, e.g., [12, 11, 16, 18]). On the other hand our model did not include indirect transmission, for realistic applications, the indirect (i.e., environment-to host) transmission it would have been better if it is included in our model and represented by saturated type functional responses, and such type of incidence forms have been used in modeling some other environmentally transmitted diseases (such as cholera [52, 53]). It would be interesting to employ saturated type incidence in our future work on brucellosis modeling, for both the autonomous and time-periodic cases.

Our study can be extended by assessing the impact of intervention strategies that minimize cattle and wildlife interactions such as maintenance of game fencing. Also the study can be strengthened by incorporating heterogeneous interaction between cattle, wildlife and humans. It is also undeniable that fitting those key model parameters with realistic seasonal data will improve our model and its applicability.

Acknowledgement

Competing Interests

The authors declare that they have no known competing financial interests or personal relationships that could have appeared to influence the work reported in this paper."

References

[1] Al Shehhi N, Aziz F, Al Hosani F, Aden B, and Blair I. Human brucellosis in the Emirate of Abu Dhabi, United Arab Emirates, 2010–2015. BMC Infectious Diseases. 2016; 16:558

[2] Hasanjani Roush MR, Ebrahimpour S. Human brucellosis: An overview. Caspian J Intern Med.2015; 6(1): 46-47.

[3] Ebrahimpour S, Youssefi MA, Karimi N, et al. The prevalence of human brucellosis in Mazandaran province, Iran. Afr J Microbiol Res 2012; 6: 4090-4.

[4] Yang L, Bi, Z-W, Kou Z-Q, et al, Time series analysis on human brucellosis during 2004–2013 in Shandong province, china. Zoonoses and Public Health; 2014.
DOI:10.1111/zph.12145.

[5] Zhang J, Sun G-Q, Sun X-D, Hou Q, Li M, et al. Prediction and control of brucellosis transmission of dairy cattle in Zhejiang Province, China. PloS ONE. 2014; 9(11): e108592.

[6] Michel AL, Bengis RG. The African buffalo: A villa for inter-species spread of infectious disease in southern Africa. Onderstepoort Journal of Veterinary Research. 2012; 79(2):1-5.

[7] Alexander KA, Blackburn JK, Vandewalle ME, Pesapane R, Baipoledi EK, et al. Buffalo, Bush Meat, and the Zoonotic Threat of Brucellosis in Botswana. PLoS ONE. 2012;7(3):e32842.
DOIi:10.1371/journal.pone.0032842.

[8] Michel AL, Bengis RG, Keet DF, Hofmeyr M, De Klerk L-M, Cross PC et al., wildlife tuberculosis in South African conservation areas: Implications and challenges, Veterinary Microbiology. 2006; 112, 91-100.

[9] Mfund I, Roskaft E. Bush meat hunting in Serengeti, Tanzania: An important economic activity to local people. International Journal of Biodiversity and Conservation. 2010; 2: 263-272.

[10] Abatih E, Ron L, Speybroeck N, Williams & Berkevens D. Mathematical analysis of the transmission dynamics of brucellosis among bison. Mathematical Methods in the Applied Sciences. 2015;38:3818-3832.

[11] Hou Q, Sun X, Zhang, Liu Y, Wang Y, Jin Z. Modeling the transmission dynamics of sheep brucellosis in Innner Mongolia autonous region, China. Mathematical Biosciences. 2013;242:51-58.

[12] Li M, Sun G, Wu Y, Zhang J, Jin Z. Transmission dynamics of multi-broup brucellosis model with mixed cross infection in public farm. Applied Mathematics and Computation. 2013; 237:582-594.

[13] Li M, Sun G, Zhang J, Jin Z, Sun X, Wang Y, Huang B, Zheng Y. Transmission dynamics and control for brucellosis model in Hingaan League Inner Mongolia, China. Mathematical Biosciences and Engineering, 2014; 11:1115-1137.

[14] Hou Q, Sun X-D. Modeling sheep brucellosis transmission with a multi-stage model in Changling County of Jilin Province, China. J. Appl. Math. Comput.
DOI 10.1007/s12190-015-0901-y

[15] Lou P, Wang L, Zhang X, Xu J, Wang K. Modelling Seasonal Brucellosis Epidemics in Bayingolin Mongol Autonomous Prefecture of Xinjiang, China, 2010-2014. BioMed Research International. 2016; Article ID 5103718:17.
Available: http://dx.doi.org/10.1155/2016/5103718.

[16] Lolika OP, Mohamed Y. A. Bakhet and Ben Saliba Lagure. Modeling Co-infection of Bovine Brucellosis and Tuberculosis: Asian Research Journal of Mathematics. 2021; 17(8): 1-13, Article no. ARJOM.73658 ISSN: 2456-477X, DOI: 10.9734/ARJOM/2021/v17i830319.

[17] Lolika OP and Mushayabasa S. Dynamics of a Reaction Diffusion Brucellosis Model: Journal of Advances in Mathematics and Computer Science. 2021; 36(8): 52-69.
Article no. JAMCS.73830, ISSN:2456-9968,DOI:10.9734/JAMCS/2021/v36i830393.

[18] Lolika OP, Mushayabasa S. On the role of short-term animal movements on the persistence of brucellosis. Mathematics, 2018, 6, 154.

[19] Qin Y, Pei X, Li M and Chai Y. Transmission dynamics of brucellosis with patch model: Shanxi and Hebei Provinces as cases. MBE, 2022; 19(6): 63966414.

[20] Abagna S, Seidu B, and CS Bornaa. A Mathematical Model of the Transmission Dynamics and Control of Bovine Brucellosis in Cattle. Hindawi: Abstract and Applied Analysis Volume 2022; Article ID 9658567, 10 pages https://doi.org/10.1155/2022/9658567.

[21] Kenne C, Mophou G, Dorville R, Zongo PA. Model for Brucellosis Disease Incorporating Age of Infection and Waning Immunity. Mathematics. 2022; 10:670. https://doi.org/10.3390/math10040670.

[22] Sun QG, Li M-T, Zhang J, Zhang W, Pei X, Jin Z. Transmission dynamics of brucellosis: Mathematical modelling and applications in China. Computational and Structural Biotechnology Journal. 2020; (18):3843-3860.

[23] Li M-T, Sun QG, Zhang Wen-Yi and Jin Z. Model-Based Evaluation of Strategies to Control Brucellosis in China. International Journal of Environmental Research and Public Health 2017.

[24] Helikumi M, Lolika OP. Global Dynamics of Fractional-order Model for Malaria Disease Transmission. ARJOM. 2022;18(9): 82-110.
Article no.ARJOM.88271ISSN: 2456-477X.

[25] Helikumi M, Lolika OP. A note on fractional-order model for cholera disease transmission with control strategies. Communications in Mathematical Biology and Neuroscience 2022; DOI: 10.28919/cmbn/7122.

[26] Helikumi M, Lolika OP, Mushayabasa S. Implications of seasonal variations, host and vector migration on spatial spread of sleeping sickness: Insights from a mathematical model. Informatics in Medicine Unlocked 2021; 24(5):100570.
DOI: 10.1016/j.imu.2021.100570.

[27] Godfroid J. Brucellosis in wildlife. Rev. sci. ettch. Off. int. Epiz. 2002; 21(2):277-286.

[28] Juan Zhang and Zhien Ma, Global dynamics of an seir epidemic model with saturating contact rate, Mathematical Biosciences Journal 2003; 185,15-32.

[29] Ariza J, Bosilkovski M, Cascio A, Colmenero JD, Corbel MJ, et al. Perspectives for the treatment of brucellosis in the 21st century: The Ioannina recommendations. PLoS Med 2007; 4(12): e317.
DOIi:10.1371/journal.pmed.0040317.

[30] Van den Driessche P and Watmough J. Reproduction number and subthreshold endemic equilibria for compartment models of disease transmission.Mathematical Biosciences, 2002; 180:29-48.

[31] Shuai Z, Heesterbeek JAP, van den Driessche P. Extending the type reproduction number to infectious disease control targeting contacts between types, J. Math. Biol. 2013; 67 (5)1067-1082.

[32] LaSalle JP. The stability of Dynamical Systems. CBMS-NSF Regional Conference Series in Applied Mathematics. 1976; vol. 25. SIAM: Philadelphia.

[33] Arriola, Leon and Hyman J, "Forward and adjoint sensitivity analysis with applications in dynamical systems", Lecture Notes in Linear Algebra and Optimization, 2005.

[34] Li J, Yang Y, Zhou Y. Global stability of an epidemic model with latent stage and vaccination. Nonlinear Analysis: Real World Applications 12(2011); 2163-21273.

[35] Altizer S, Dobson A, Hosseini P, Hudson P, Pascual M, et al. Seasonality and the dynamics of infectious diseases. Ecology Letters 2006; 9: 467-484.

[36] Dowel SF. Seasonal Variation in Host Susceptibility and Cycles of Certain Infectious Diseases. Emerging Infectious Diseases 2001; 7: 369-374.

[37] Aune K, Rhyan JC, Russell R, Roffe TJ, Corso B. Environmental persistence of Brucella abortus in the Greater Yellowstone Area. Journal of Wildlife Management, 2012;76: 253 - 261.

[38] Beauvais W, Musallam I, Guitian J. Vaccination control programs for multiple livestock host species: an age-stratified, seasonal transmission model for brucellosis control in endemic settings. Parasites and Vectors. 2016;9:55.

[39] Wang W and Zhao X-Q . Threshold dynamics for compartment epidemic models in periodic environments. Journal of Dynamics and Differential Equations. 2008; 20:699-717.

[40] Zhang F, Zhao X-Q. A periodic epidemic model in a patchy environment.J. Math. Anal. Appl. 2007; 325,496-516.

[41] Smith HL, Walman P. The Theory of the Chemostat. Cambridge University Press, Cambridge, 1995.

[42] Thieme HR. Convergence results and a Poincare-Bendison trichotomy for asymptotical autonomous differential equations. J. Math. Biol. 1992; 30, 755-763.

[43] Silva CJ, Maurer H, Torres DFM. Optimal control of a tuberculosis model with state and control delays. Math. Biosci. Eng. 2017; 14, 321-337.

[44] Di Liddo A . Optimal control and treatment of infectious diseases. the case of huge treatment costs. Mathematics 2016; 4(2):21.

[45] H. Abboubakar, KouchrGuidzava A, Yangla J. et al.,Mathematical modeling and projections of a vector-borne disease with optimal control strategies: A case study of the Chikungunya in Chad, Chaos, Solitons and Fractals (150) 2021; 111197.

[46] Abboubakar H , Kamgang JC , Nkamba LN , Tieudjo D . Bifurcation thresholds and optimal control in transmission dynamics of arboviral diseases. J Math Biol 2018; 76(12):379427.

[47] Abboubakar H , Kamgang JC . Optimal control of arboviral diseases. In: Pro- ceedings of CARI; 2016. p. 445.

[48] Lenhart S , Workman JT . Optimal control applied to biological models. CRC press; 2007.

[49] Fleming WH, Rishel RW. Deterministic and stochastic optimal control, Springer Verag, New York, 1975.

[50] Pontryagin LS, Boltyanskii VT, Gamkrelidze RV, Mishcheuko EF. The mathematical theory of optimal processes, Wiley, New Jersey, 1962.

[51] Agriculture, Forestry and Fisheries, Republic of South Africa. Interim Brucellosis Manual (2013).

[52] C.T. Codeco, Endemic and epidemic dynamics of cholera: the role of the aquatic reservoir, BMC Infect. Dis. 1 (2001) 1.

[53] Mukandavire Z, Liao S, Wang J, Gaff H, Smith DL, Morris JG, Estimating the reproductive numbers for the 20082009 cholera outbreaks in Zimbabwe, Proc. Natl. Acad. Sci. 2011;108:8767-8772.

Peer-review history:
The peer review history for this paper can be accessed here (Please copy paste the total link in your browser address bar)
https://www.sdiarticle5.com/review-history/90620